Available online at www.sciencedirect.com

ScienceDirect

journal homepage: www.elsevier.com/locate/he

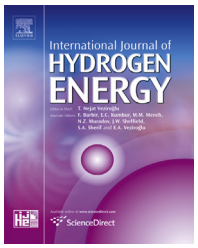

Sensitivity analysis of stack power uncertainty in a PEMFC-based powertrain for aircraft application

G. Correa [a,*], F. Borello [b], M. Santarelli [c]

[a] Centro de Investigaciones y Transferencia de Catamarca (CITCA), CONICET-UNCA, Facultad de Ciencias Exactas y Naturales (UNCa), Maipú 662 – 4700, San Fernando del Valle de Catamarca, Argentina

[b] Politecnico di Torino, Departmant of Mechanical and Aerospace Engineering, Corso Duca degli Abruzzi 24, 10129 Torino, Italy

[c] Politecnico di Torino, Department of Energy, Corso Duca degli Abruzzi 24, 10129 Torino, Italy

ARTICLE INFO

Article history:
Received 31 March 2015
Received in revised form
15 May 2015
Accepted 19 May 2015
Available online 4 July 2015

Keywords:
PEM fuel cell
Sensor reliability
Sensitivity analysis
Aircraft power system
Dynamic model

ABSTRACT

Experimental data concerning the reliability of fuel cell systems (FCS) in aviation are still unavailable to technical community, while assessing reliability of a component or a whole system represents a fundamental aspect that allows a new technology to be introduced in a high safety system such as an aircraft. The main aim of this paper is to show a method to estimate the reliability of an aircraft power system based on a hydrogen fuel cell, mainly for design purposes. The method is based on a high-order adaptive response surface technique, coupled with a dynamic model of the aircraft power system, and it is applied to the failure event represented by an incorrect power supply due to the failure of sensors of the control system of the powertrain. The most important advantage of the proposed method is the low computational effort it requires. The result is a ranking of the most critical sensors to be considered in the design phase of the power system and demonstrate that accurate temperature sensors and sensor calibration are of dramatic importance for the control of the stack power, in case of powertrain based on PEM fuel cell systems.

Introduction

In parallel with the increasing interest in renewable fuels, high efficiency powertrain technologies start to be considered, such as fuel cell technologies. The high efficiency and environmental advantages of fuel-cell technology have generated an increasing interest in the aviation community. So far, the use of fuel-cell systems for propulsion of manned aircraft has been adequately demonstrated only in three projects: Boeing fuel-cell demonstrator airplane [1], the Antares DLR-H2 fuel-cell aircraft project [2], and the ENFICA-FC project [3].

Among the various types of Fuel Cells, the PEMFC technology has found widespread use, especially in vehicular application [4]. Instead, only two fuel cell technologies could be considered for aviation applications: PEMFC and SOFC,

Abbreviations: act, Activation; an, Anode; Amb, Ambient; ca, Cathode; CDF, Probability distribution function; conc, Concentration; HEX, Heat Exchanger; FC, Fuel cell; MC, Monte Carlo; Mem, Membrane; ohm, Ohmic; RSM, Response surface method; st, Stack; WC, Water cooling (deionizer water).

* Corresponding author. Tel.: +54 93513337718.
E-mail address: correa.gabriel@conicet.gov.ar (G. Correa).
http://dx.doi.org/10.1016/j.ijhydene.2015.05.133

Notations

A	Area, [m^2]
A_c	Cell active surface, [cm^2]
c_v	Water concentration, [mol/cm^3]
D	Diffusion coefficient, [cm^2/s]
E_0	Open Circuit Voltage, [volts]
C,Cp	Specific heat, [J/(kg K)]
F	Faraday number, [C/mol]
G	Mass flow rate, [kg/s]
g	Gibbs free energy, [W]
h	Mass specific enthalpy of the mass flow, [J/kg]
i	Current density, [A/cm^2]
I	Current, [A]
l	Electrode perpendicular distance
m	Total mass, [kg]
N_v	Net water flow [$mol/(s\ cm^2)$]
n_c	Number of cells in series in the PEMFC stack
n_d	drag coefficient [-]
P	Pressure, [bar]
P^{sat}	Saturation pressure, [bar]
R	Universal gas constant, [J/(mol °K)]
R_a	Propeller radius, [m]
S_{HEX}	Frontal surface of the heat exchanger, [m^2]
r	Resistance, [$\Omega\ m^2$]
T_r	Propeller thrust, [kg]
T	Temperature, [°K]
t_m	Membrane thickness, [cm]
V_c	Cell voltage, [V]
V_∞	Onset flow velocity, [m/s]
x_i	mole fraction of constituent i [-]
Wel	Electric power produced by the stack, [W]

Greek letters

α^{el}	electrode transfer coefficients [-]
Φ	Heat transfer, [W]
η	over-voltage, [V]
ρ	Air density, [kg/m^3]

while the AFC systems have been used for space, but issues with poisoning by CO and CO_2 would eliminate applicability for general aviation. The MCFC technology [5,6] is the less suitable for transport application due to its low power density and the adoption of the electrolyte in molten phase; they are instead the cells with the higher rate of installation worldwide in the stationary applications, mainly at the level of power plants, with also the largest size power plant so far in operation (58.8 MW in Korea, produced by Posco energy).

Some of the key advantages and some disadvantages of PEMFC systems over the other competitive types of FCs can be specified as follows [7,8]: They provide high power density, high chemical-to-electrical energy conversion efficiency, and fast and easy start-up and operated a low temperature. The disadvantages are: they are very sensitive to impurities of hydrogen, need humidification units of reactive gases and use very expensive catalyst (platinum) and membrane (solid polymer).

In the early phases of the introduction of a new technology in highly controlled systems, information about the elements that most affect the reliability is critical for the designer. Unfortunately the reliability of new technologies is rarely known, because of an insufficient pool of data, both in terms of quantity and representativeness. In particular, for new device such as fuel cells, the failures data are always very difficult to obtain, due to the prolonged test periods required [9].

Some authors that works in fault detection and diagnosis found that some common fault sources of improper operation and control of fuel cell systems are sensors system (spurious o mal function) [10–13].

Several authors such as Mawardi and Pitchumani [14], Placca et al. [15] and Noorkami et al. [16] have worked on the study of uncertainties with the idea of assessing the effects on the performance of the fuel cell.

Mawardi and Pitchumani [14] develops a sampling-based stochastic model to elucidate the effects of uncertainty in operating cell temperature, anode pressure, and cathode pressure on the variation of power density. A one-dimensional non isothermal model is used to simulate the fuel cell operation for each sample. Based on the stochastic convergence analysis, a sample size of 100 was selected.

Noorkami et al. [16] estimate the expected level of uncertainty in polarization performance based on a given uncertainty in the temperature of the system (spatial and temporal). A simple lumped mathematical model is used to describe PEMFC performance under temperature uncertainty. An analytical approach gives a measure of the sensitivity of performance to temperature at different nominal operating temperatures and electrical loadings. The uncertainty assessment method used in this work is a direct Monte Carlo simulation.

The work of Placca et al. [15] focuses on the statistical analysis of the output voltage of a semi-empirical proton exchange membrane fuel cell model, introducing a degradation rate on the cell active area. The statistical analysis is performed by a quadratic response surface method and ANOVA with 1000 samples. The authors are able to define sensitivities and statistical description of the output, however the implemented statistical method requires great computational effort for models that require high number of variables.

In this work the authors present a method of failure analysis of fuel cell-based powertrain in case of aircraft application that can be used during the design phase. The method is general enough to be applied to different performance parameters of the targeted system, and to different sources of failure (here described as uncertainty in the performance of a component).

The novelties of the presented work are twofold: first of all the problem is analyzed from the point of view of the fault of sensors; this is due to the fact that the motivations of the work is to provide a tool to define the required equipment of the fuel cell system in an aeronautical application, where safety is often achieved by redundancies. Sensitivities can provide a useful measure of the relative importance of each sensor.

The second innovative aspect of the work is the used probabilistic method: an adaptive response surface is used to accurately predict the model outcome and to be processed by estimation methods (Monte Carlo, FORM, SORM or any other method). The method is able to evaluate the most suitable form for the response surface and this allows an easier

implementation of a high number of random variable and a save in computational effort.

The Fig. 1 shows the PEMFC system, composed of the FC stack and the balance of plant (a heat exchanger, a pump and a water tank reservoir) furthermore shows the sensors configuration. The analyzed sensor are: Anode inlet temperature (*Tan_in*), Anode inlet pressure (*Pan_in*), Anode inlet mass flow (*Gan_in*), Cathode inlet pressure (*Pca_in*), WC inlet temperature (*Twc_in*), WC inlet mass flow (*Gwc_in*), Ambient temperature (*Tamb*), Cathode inlet mass flow (*Gca_in*) and Cathode inlet temp (*Tca_in*). From the FC control point of view, the sensor signals could be treated as input parameters of the control system.

Being the fuel cell a power generation device, one of the most important parameter to control is (from an uncertainty analysis point of view) the stack power of the system, since it is the measure of the performance of the whole system. For this reason the fuel cell stack power was chosen as the system response to be studied by probabilistic investigation, while the failures are represented by the misreading of the sensors used by the logic of control to drive the fuel cells.

The problem was approached coupling a dynamic model of the aircraft power system based on fuel cell, and an adaptive high order method for response surface generation. This approach has the advantage to use a complex dynamic model that requires a significant computational effort, but a very fast probabilistic method that allows to evaluation the behavior of the model with sufficient accuracy without solving it for every sample point of the random experiment space, as in standard Monte Carlo simulations. The dynamic model was not only validated by open literature case studies, but also, for the first time as far as the authors are aware of, by a real world application: the telemetry data provided by the six flights of the ENFICA-FC aircraft were used to tune and verify the correct behavior of the mathematical model.

The result is a ranking of the most critical sensors: this information can be used by the designer, as an example, to consider the proper redundancy of sensors or the appropriate handling of the data by the control software.

Description of the power system of the 2-seater airplane powered by fuel cells

The fuel cell system was installed in the light sport aircraft RAPID 200, manufactured by Sky Leader Aircraft. The requested mission performance is reported in Ref. [17], however can be summarized as follow:

1. Take-off (max 40 kW);
2. Climbing up to 1000 m with a rate of climb of 2.5 m/s (max 40 kW);
3. Cruising over the airport at approximately 150 km/h for 40 min (max 20 kW);
4. Descending and landing;

The required power for each phase of the mission is shown in Fig. 2.

A full description of the power system could be found in Ref. [17], but it is briefly described here.

A hybrid battery/fuel cell system was chosen: the fuel cell system able to provide 20 kW of net unregulated power and two Li–Po battery packs supply 20 kW for 18 min. Although the main motivation for introducing the hybridization in fuel cell systems in aircraft applications is reduce the overall weight of the system, the benefits are not limited to that. The use of a second source of energy could work as an emergency power source, as in the case of the failure of the fuel cell, in order to allow pilot to land safely. To guarantee the necessary performance, the brushless electric motor relies on air cooling and this has led to a saving in weight as a water cooling system is no longer required. The hydrogen storage and distribution system consists of two tanks of 26 L each and they were manufactured for a working pressure of 350 bar (leading to a total H_2 mass capacity of 1.2 kg).

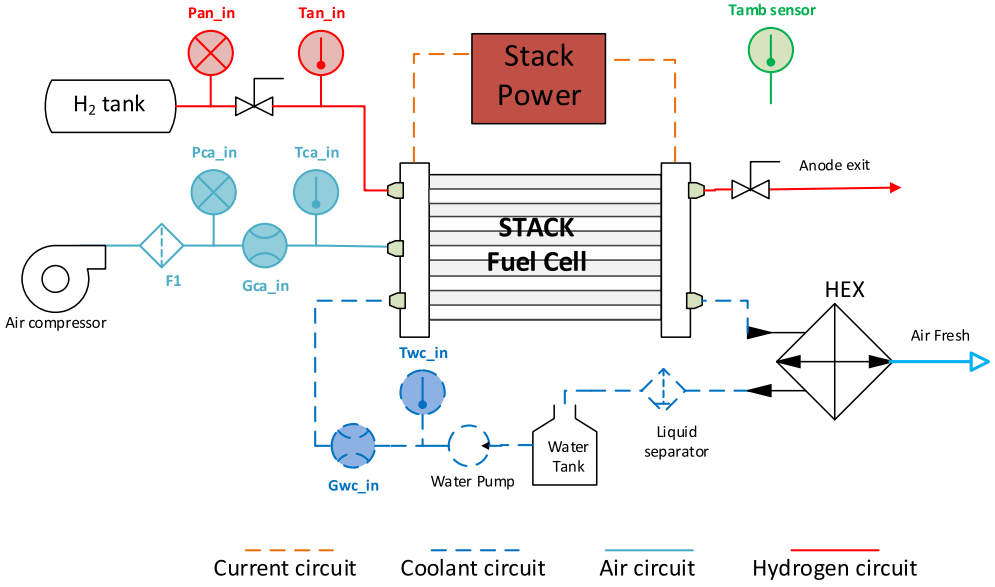

Fig. 1 – General scheme of the sensor signals.

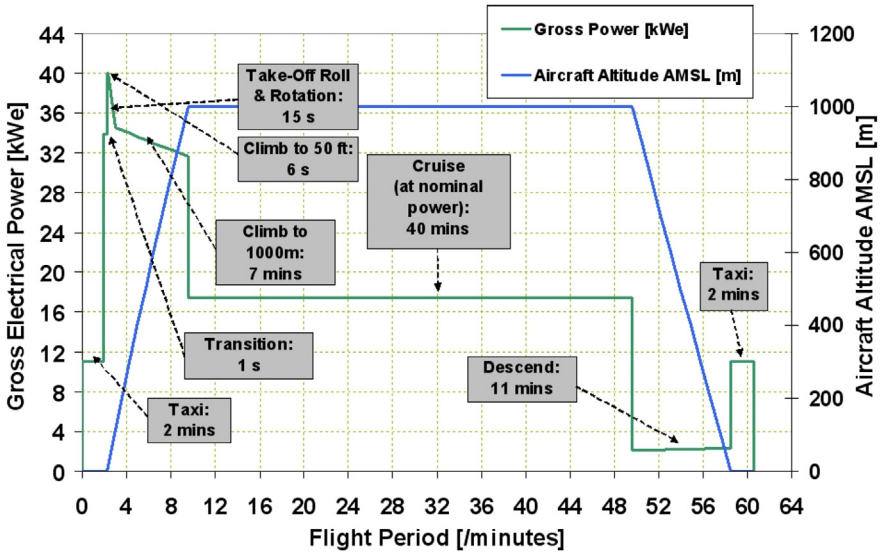

Fig. 2 – Mission and required gross power profiles.

The FCS, designed and built by the UK-based Intelligent Energy Company (EC200-168), includes two separate PEMFC stacks electrically connected in series. Each stack is composed of a series of 168 cells. The maximum power output of the systems is approximately 20 kW net or 24 kW gross at approximately 220 V. The membranes have an active area of 200 cm^2. A complete description of the FCS and the Balance of Plant is reported in Ref. [18].

Model description

A PEMFC stack dynamic model, taking into account the main electrochemical, fluid-dynamic and thermal processes is briefly described. The code (see Fig. 3) is based on a existed dynamic model of the fuel cell and balance of plant [19] coupled with the model of the propeller, and taking into account geometrical parameters of the aircraft [20,21]. The input of the code needs data of the external environment (ambient temperature and pressure), the mission profiles (altitude and speed) and the propeller characteristic curves (obtained from Ref. [22]). As it is shown in Fig. 3, the fluid dynamic model is able to provide the instantaneous amount of fresh air wetting the heat exchanger active surface where it cools the waste water–air mixture from the fuel cell stacks. The cooled waste water returns to the water tank to be re-used. In order to obtain the stack power output, the temperature of the water leaving the heat exchanger, the temperature of the water entering fuel cell stack and the temperature at the cathode side outlet have to be computed. Moreover, since the voltage depends on the reactant pressures at the catalyst layer, the concentration needs to be described as a function of the cell's operating condition.

The code is based on physical inputs (Table 1) and fixed parameters assumed from specific literature (Table 2), and several assumptions were made to prepare these models: all gases obey the ideal gas law; when the relative humidity of the gas exceeds 100%, vapor condenses into the liquid form, in order to obtain a computationally non-intensive ideally analytical model an 1D description (One-dimensional treatment) has been developed.

The model was validated on the basis of a thorough demonstration session on an ultra-light aircraft, performed in the framework of the ENFICA-FC project, during which an extensive test campaign of six flights was performed. An initial sensitivity analysis of the flight results is described in Ref. [20], while the validation of the model through experimental flight data is reported in Ref. [23]. The literature data were obtained from publications written by Intelligent Energy (IE), which as previously mentioned, is the manufacturer of the Fuel Cell [24,25]. The lower and upper limits of the design parameters were selected based on the basis of a parametric study of PEM fuel cells found in Muller et al. (2006) [26].

Electrochemical model

In order to compute the fuel cell voltage, the open circuit voltage (OCV) of the fuel cell is defined (E_0). When net current is extracted from the fuel cell, a change in the equilibrium conditions occurs and over-voltages take place. Activation overpotential is expressed by the Butler–Volmer equation [27,28] and could be written in explicit form with the electrode overpotential, assuming that the symmetry factors on the reaction on an electrode are equal [27,29]. The ionic resistance of the membrane is related to the operating temperature, but especially to the degree of humidification of the membrane [29]. In Table 3 are summarized the key equations of electrochemical model.

Mass balance model

The cathode and anode flow behavior have been described on the basis of the model presented by Pukrushpan et al., 2004 [31]. The gas transport in the gas diffusion layer is computed, and the water transport across the membrane can then also be analyzed assuming that the fuel is humidified and that the effective water vapor pressure of the anode is 50% of the

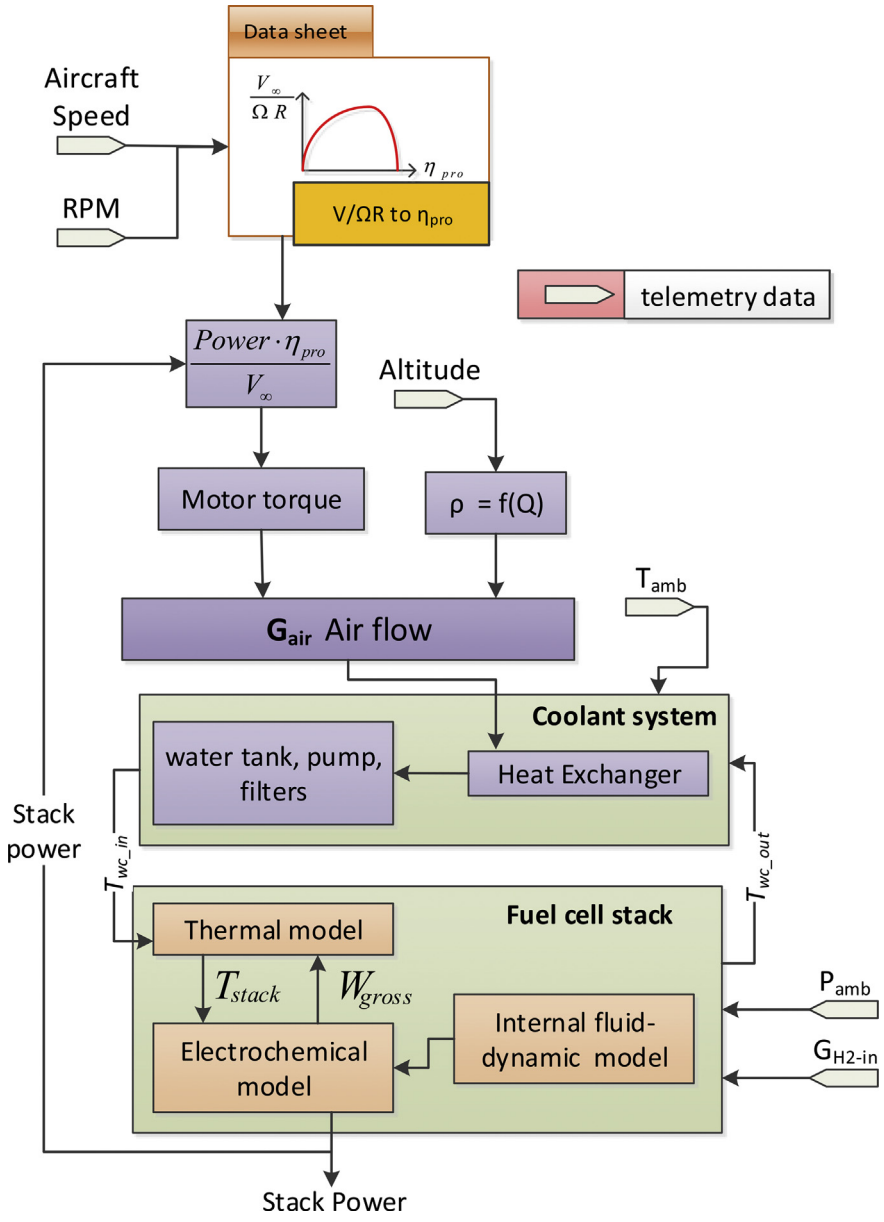

Fig. 3 – Schematic of the PEMFC-based system model coupled with fresh air model.

saturated vapor pressure [32]. The binary diffusion coefficients D_{H2O-H2}, D_{O2-N2} and D_{O2-H2O}, have been determined from the Slattery-Bird equation as outlined in Ref. [33]. The equivalent water diffusion coefficient in the membrane (D_w) and the electro-osmotic drag coefficient (n_d) have been taken from experimental data and curve fits from Ref. [30]. In Table 4 the key equations are shown.

Table 1 – System physical input.

Inputs	Variable name	Unit
Power required	W_{el_req}	[kW]
Ambient temperature	T_{amb}	[K]
Ambient pressure	P_{amb}	[bar]
Air inlet pressure	P_{air_in}	[bar]
Hydrogen inlet pressure	P_{H2_in}	[bar]
Hydrogen inlet mass flow rate	G_{H2_in}	[kg/s]

Thermal model

The thermal model of the stack is briefly described here (Table 5), but a complete description could be found in Ref. [19].

Inlet fresh air flow HEX model

In order to develop an engineering model for inlet fresh air flow inlet to the HEX, several approximations of real fluid mechanics are required. In a previous work for the authors [20], a simplified model that predicts the behavior of the heat exchanger air intake is developed, even if the effect of the propeller swirl wake and the pressure losses (due to skin

Table 2 – Fixed assumed parameter values.

Name	Parameter (π_i)	Value	
Anode exchange current density	i_{0an}	0.2	A/cm^2
Anode pressure inlet	p_{an_in}	101,325	Pa
Capacitance	C	0.002	F/cm^2
Cell active surface	A	200	cm^2
Convective heat transfer coefficient-FC body to ambient	$h_{cell\text{-}amb}$	20	W/(m^2 K)
Convective heat transfer coefficient-Water tank to ambient	$h_{Wtank\text{-}amb}$	150	W/(m^2 K)
Frontal surface heat exchanger	S_{HEX}	0.042	m^2
Membrane thickness	t_m	0.0025	Cm
Number of cells in series in the PEMFC stack	N_{cell}	336	
Parameter of the heat transfer coefficient	K_h	9000	
Surface area-FC body to ambient	$A_{cell\text{-}amb}$	0.8	m^2
Surface area-Water tank to ambient	$A_{Wtank\text{-}amb}$	0.3	m^2
Surface area-Heat exchanger to ambient	$A_{HEX\text{-}amb}$	0.6	m^2
Thermal capacity of fuel cell body	mC_{st}	24,000	J/K
Thermal capacity of coolant	mC_{WC}	8000	J/K
Thermal capacity of Heat exchanger	mC_{HEX}	25,000	J/K

Table 3 – Key equations of electrochemical model.

Description	Equation	Ref
FC voltage	$V_{FC} = E_0 - \eta_{act} - \eta_{ohm} - \eta_{conc}$	
Open circuit voltage	$E_0 = -\frac{\Delta\bar{g}(T_{st},p_0)}{nF} + \frac{RT_{st}}{nF}\ln\left(\frac{P_{H_2}P_{O_2}^{0.5}}{P_{H_2O}}\right)$	
Activation loss at the electrodes	$\eta_{act,cat} + \eta_{act,an} = \eta_{act} = \frac{R\cdot T}{2\cdot F}\sinh^{-1}\left(\frac{i}{2\cdot i_{0,an}}\right) + \frac{R\cdot T}{0.5\cdot F}\sinh^{-1}\left(\frac{i}{2\cdot i_{0,c}}\right)$	[27–29]
Cathode exchange current density	$i_{0,c} = T^2(552\times10^{-9}) + T_{st}(-321\times10^{-6}) + 0.04674$	[23]
Ohmic loss	$\eta_{ohm} = r_{ohm}\cdot i \rightarrow r_{ohm} = r_{elec} + r_{ion} \rightarrow r_{elec} << r_{ion}$	
Ionic resistance	$r_{ion} = r_m = \frac{t_m}{(5{,}139\times10^{-3}\cdot\lambda_m - 3{,}26\times10^{-3})\exp\left(2416\cdot\left(\frac{1}{273}-\frac{1}{T_{stack}}\right)\right)}$	[30]

Table 4 – Key equations of mass balance model.

Description	Equation	Ref
Hydrogen effective partial pressure	$p^*_{H_2} = 0.5\cdot p^{sat}_{H_2O}\left[\frac{1}{x^{channel}_{H_2O}\exp\left(\frac{RT}{pan2F}\frac{I_{st}l_{an}}{D_{H_2O,H_2}}\right)} - 1\right]$	[32,34,35]
Vapor effective molar fraction	$x^*_{H_2O} = x^{channel}_{H_2O}\exp\left(\frac{RT}{p_{ca}4F}\frac{I_{st}l_{ca}}{D_{H_2O,O_2}}\right)$	
Nitrogen effective molar fraction	$x^*_{N_2} = x^{channel}_{N_2}\exp\left(\frac{RT}{p_{ca}4F}\frac{I_{st}l_{ca}}{D_{N_2,O_2}}\right)$	
Oxygen effective partial pressure	$p^*_{O_2} = p^{sat}_{H_2O}\left[\frac{1-x^*_{N_2}}{x^*_{H_2O}} - 1\right]$	
Net water flux rate across the membrane	$N_{v,memb} = n_d\frac{I_{st}}{F} - D_w\frac{c_{v,ca}-c_{v,an}}{t_m}$	[30,33,35–39]
Total mass flow rate across the membrane	$G_{v,memb} = N_{v,memb}\cdot M_v\cdot A_{FC}\cdot n$	
Average water in cathode and anode	$a_{ca} = \frac{p_{v,ca}}{p_{sat,ca}} \ldots a_{an} = \frac{p_{v,an}}{p_{sat,an}}$	
Average water activity	$a_m = \frac{a_{an}+a_{ca}}{2}$	
Membrane average water content	$\lambda_m = \begin{cases} 0.043 + 17.81a_m - 39.85a_m^2 + 36a_m^3 \rightarrow 0 < a_m \le 1 \\ 14 + 14(a_m - 1) \rightarrow 1 < a_m \le 3 \end{cases}$	

Table 5 – Key equations of thermal model.

Description	Equation	Ref
Rate of change of energy inside the control volume	$mC_{st}\cdot\frac{dT_{st}}{dt}=\sum_i \pm G_i\cdot h_{ph,i}-\left\lvert\Phi_{Conv}^{Amb}\right\rvert-\left\lvert\Phi_{Conv}^{WC}\right\rvert+\Phi_{source}$	
Reaction enthalpy rate	$\sum_i \pm G_i\cdot h_{ph,i}\stackrel{i}{=}\sum_i (G_{i,IN}\cdot Cp_{i,IN}\cdot T_{i,IN}-G_{i,OUT}\cdot Cp_{i,OUT}\cdot T_{i,OUT})$	
Heat convection to the external environment	$\left\lvert\Phi_{Conv}^{Amb}\right\rvert=A_{stack}^{amb}\cdot h_{conv}^{cell-amb}(T_{st}-T_{amb})$	
Heat generation in the stack	$\Phi_{source}=n_c\cdot i\cdot A_c\cdot\left[\frac{-T_{st}\cdot\Delta\bar{s}_{react}}{2\cdot F}+\sum_j \eta_j\right]$	
Heat flux rate transfer – Fuel cell body to WC	$\left\lvert\Phi_{Conv}^{WC}\right\rvert=A_{stack}^{WC}\cdot h_{conv}^{WC-st}(T_{st}-T_{WC}^{0})$	

friction) are neglected. These effects were simulated in a CFD model [21]. During the operating condition, the pressure drop at the heat exchanger is equal to the pressure prevalence provided by the air intake as indicated in Eq. (1)

$$G_{air}^2\cdot k1+G_{air}\cdot k2+k3=\frac{1}{2}\rho\cdot V_\infty^2+\frac{Tr}{\pi\cdot R_a^2}-\frac{1}{2}\rho\left(\frac{G_{air}}{S_{HEX}}\right)^2 \quad (1)$$

where k_1, k_2, k_3 are empirically determined constants [20], and G_{air} is the air inlet flow rate.

Uncertainty and sensitivity analysis methods

The approach to failure analysis is usually deterministic, in the sense that the random nature of the failure events is mathematically or numerically treated so that it can be expressed by a deterministic value [11]. The problem can be also approached by probabilistic methods that describe the basic parameters through probability distributions, such as reliability-oriented techniques. These techniques can be divided in two wide categories: numerical simulation (Monte Carlo method and related variance reduction techniques) and limit state approximation and variables transformation (First and Second Order Reliability Methods). These two categories are representative of two opposite approaches: the first methods do not introduce approximations in the probabilistic representation of the model and perform a probabilistic evaluation through an accumulation of deterministic analysis, resulting very time consuming. The second methods introduce a wide range of probabilistic approximations both for the basic random variables and for the probabilistic space in order to transform the problem in a special case for which some very peculiar properties hold; those properties allow to evaluate probabilities very quickly, but with approximations whose entity depends on the differences between the original model and the transformed one.

A good compromise could be obtained by response surface methods; they are based on the approximation of the real model by an explicit mathematical function, usually obtained by best-fitting a proper number of strategically chosen points of the original model.

In this paper, the high order response surface method presented in Ref. [40] is applied to the FC model; the method builds the response surface through high order polynomials whose order is automatically adapted to the model itself.

The method can be briefly summarized in three steps:

- Determination of the first approximation dependency between the model and each single random variable in a $\pm 6\sigma$ range of probability;
- Determination of the polynomials general structure exploiting the results of the previous step;
- Generation of the model samples by Latin Hypercube Sampling [41] and final regression by Single Value Decomposition technique [42].

The main advantages of the present method are the following: as in every RSM, the original model evaluations are far lesser than the ones required by a Monte Carlo simulation; moreover the presented method, contrary to the relocation techniques often used in RSM, keeps the full control on the required simulation since the method accuracy improvement doesn't depend on a convergence, but on the adaptive high order polynomials. The method doesn't introduce any approximation in the random variable space, so that the basic random variables are correctly represented in the low probability density regions. Moreover a single execution can generate different response surface for different model outputs, optimizing the original model evaluations done in the first step and in the third step.

Sensitivity analysis of the fuel cell system model: results and discussion

As mentioned above, the methodology is applied to the illustrative case study that has the stack power as the main performance parameter and the sensor misreadings as the basic random events that represent failures. The produced power and the sensor readings are strongly connected by the control software of the fuel cell system; a failure of one or more sensors can severely compromise the control logic and hence the functionality of the entire power system. The desired result is a ranking of the importance of the effect of each sensor to the selected performance parameter (the stack power in this case).

Sensitivities represent the contribution of the uncertainty of a single random variable to the global uncertainty of the output random variable; this contribution can be interpreted as the relative importance of one variable with respect to another one, in the sense that a variable that mostly contributes to the global uncertainty is more important because its failure has a stronger effect on the performance parameter. The computation of the sensitivity of the stack power with respect to the main model parameters (π_i) is performed through the expression in Eq. (2), where $W_{el\text{-}Stack}$ is stack electric power.

Table 6 – Spurious signal distribution.

Name	Variable	Variable poly	Distribution	Mean value	Standard deviation
Anode inlet temperature	T_{an_in}	X_1	Normal	1	0.015
Anode inlet pressure	P_{an_in}	X_2	Normal	1	0.015
Anode inlet mass flow	G_{an_in}	X_3	Normal	1	0.015
Cathode inlet pressure	P_{ca_in}	X_4	Normal	1	0.015
WC inlet temperature	T_{wc_in}	X_5	Normal	1	0.015
WC inlet mass flow	G_{wc_in}	X_6	Normal	1	0.015
Ambient temperature	T_{amb}	X_7	Normal	1	0.015
Cathode inlet mass flow	G_{ca_in}	X_8	Normal	1	0.015
Cathode inlet temp	T_{ca_in}	X_9	Normal	1	0.015

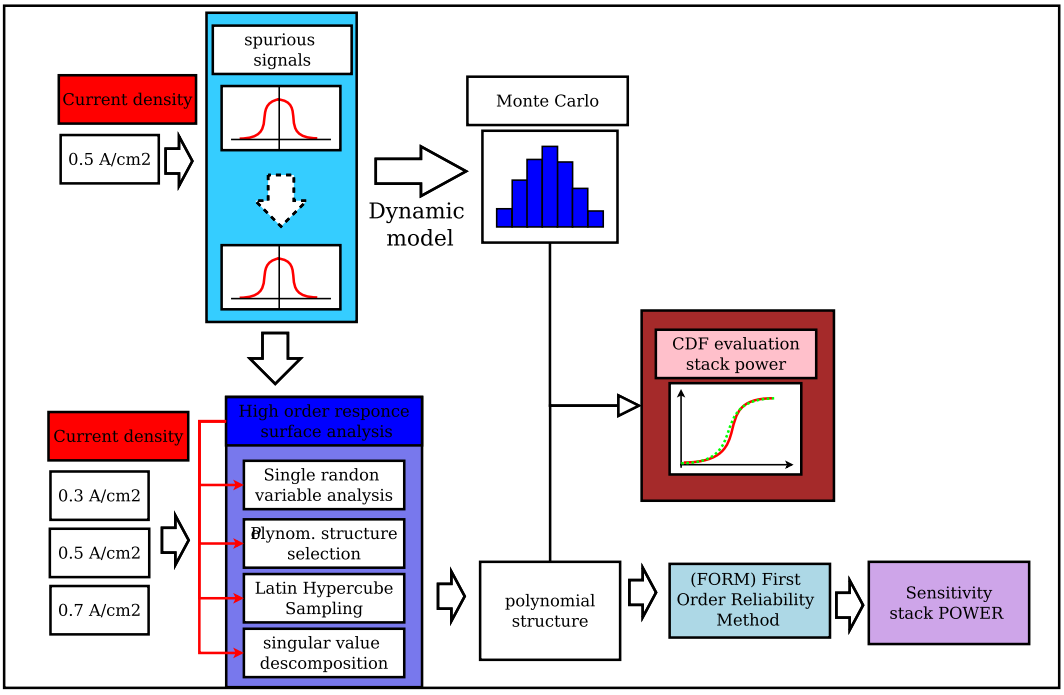

Fig. 4 – General scheme of the sensitivity/uncertainly process.

$$\vec{S} = \frac{\nabla W_{el-Stack}(\pi_i)}{\sqrt{\sum_{i=1}^{n}\left(\frac{\partial W_{el-Stack}}{\partial \pi_i}\right)^2}} \rightarrow W_{el-Stack} = f(\pi_i) \quad (2)$$

In order to compare the importance of the variables, each one has received the same probabilistic description in terms of an equal probability distribution function; in this study a normal distribution with a mean value of 1 and a standard deviation of 0.015 was chosen (Table 6).

Each input of the system has been multiplied by a source of uncertainty, as described in Fig. 4, in order to simulate the random (or spurious) signal. The distribution of each input is shown in Fig. 5.

In the subsequent steps of the procedure, the probabilistic code developed in Ref. [40] has been integrated with the model developed in this paper, in order to develop the response surface that is used for probabilistic sensitivity analysis.

Applying the previously described procedure, a polynomial structure is obtained, and of course this can be done for different current density. As an example the structure for 0.5 A/cm2 is reported:

$$\begin{aligned} P = {} & c_0 + c_1X_1 + c_2X_2 + c_3X_3 + c_4X_4 + c_5X_5 + c_6X_6 + c_7X_7 + c_8X_8 + c_9X_9 + \\ & + c_{10}X_1^2 + c_{11}X_1X_2 + c_{12}X_1X_3 + c_{13}X_1X_4 + c_{14}X_1X_5 + c_{15}X_1X_6 + c_{16}X_1X_7 + c_{17}X_1X_8 + \\ & + c_{18}X_1X_9 + c_{19}X_2X_3 + c_{20}X_2X_4 + c_{21}X_2X_5 + c_{22}X_2X_6 + c_{23}X_2X_7 + c_{24}X_2X_8 + \\ & + c_{25}X_2X_9 + c_{26}X_3X_4 + c_{27}X_3X_{5c} + c_{28}X_3X_6 + c_{29}X_3X_7 + c_{30}X_3X_8 + c_{31}X_3X_9 + \\ & + c_{32}X_4^2 + c_{33}X_4X_5 + c_{34}X_4X_6 + c_{35}X_4X_7 + c_{36}X_4X_8 + c_{37}X_4X_9 + c_{38}X_5X_6 + \\ & + c_{39}X_5X_7 + c_{40}X_5X_8 + c_{41}X_5X_9 + c_{42}X_6X_7 + c_{43}X_6X_8 + c_{44}X_6X_9 + c_{45}X_7^2 + \\ & + c_{46}X_7X_8 + c_{47}X_7X_9 + c_{48}X_8^2 + c_{49}X_8X_9; \end{aligned} \quad (3)$$

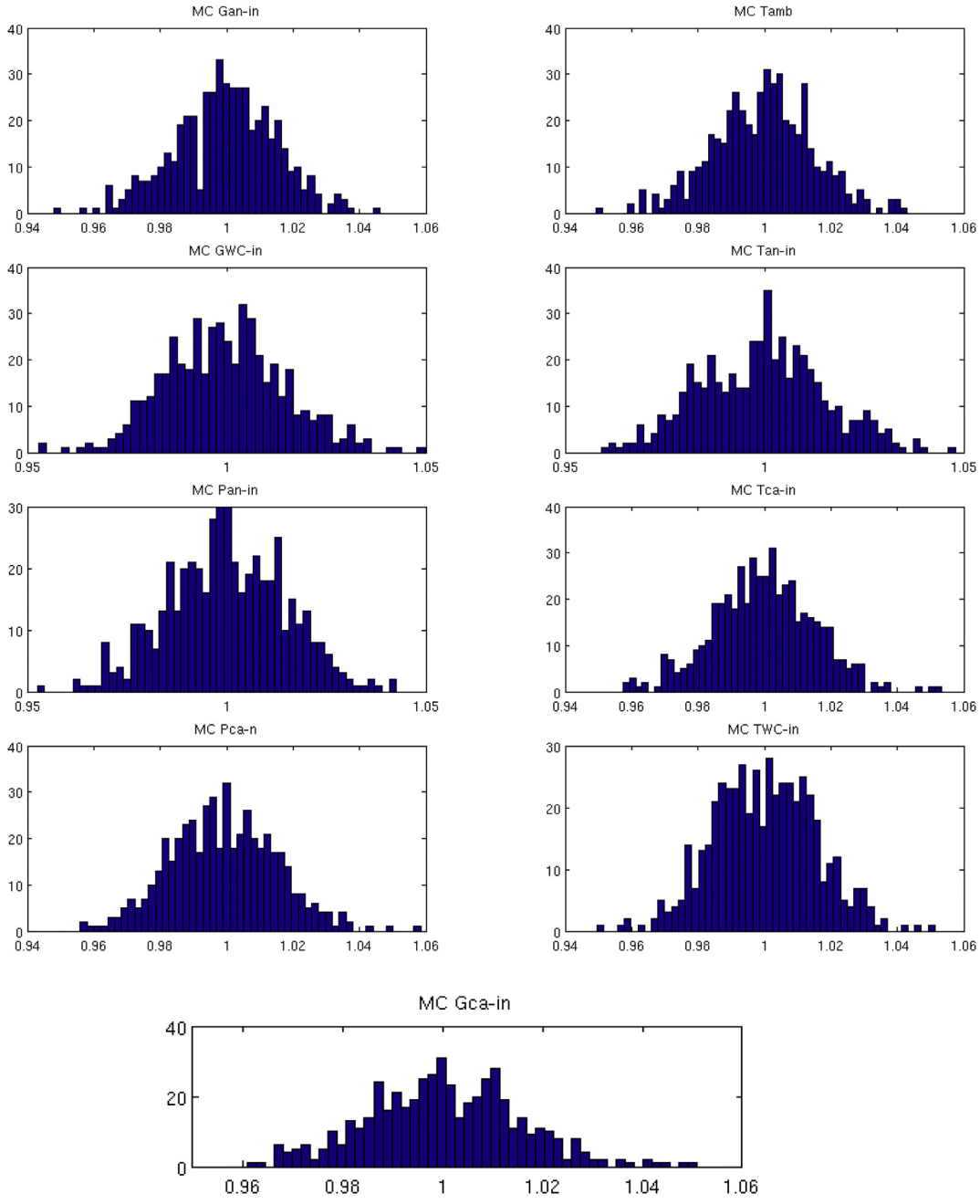

Fig. 5 – Signal distributions.

In order to compute the 50 unknown coefficients, the code generates 86 sample points via Latin Hypercube Sampling and performs the regression through the Singular Value Decomposition technique. The results are reported in Table 7.

The probabilistic sensitivity analysis is carried out for different values of current densities (0.3, 0.5 and 0.7 A/cm^2) using the response surface generated by the methodology shown in the previous sections; the 0.5 A/cm^2 case has been used as the test case for the response surface generation comparing it to a crude Monte Carlo simulation. In Fig. 6 the comparison between the CDF evaluated by Monte Carlo simulation (10^5 model evaluations) with the simulation done through the response surface (model evaluations and 10^5 response surface evaluations) of the stack power, is respectively reported. The comparison shows good agreement between the two methods.

After verifying that the methodology is reliable, the RSM analysis can be extended getting response surfaces for different current densities, as shown in Fig. 4.

The most important advantage of RSM is the computational effort it requires; for model of complex systems whose analysis is time consuming and accumulation of thousands of simulations for reliability analysis may become unacceptable.

Sensitivities are a function of the value of the CDF; each point of the CDF presents a set of sensitivities to the basic random variables. In this case study the sensitivity values

Table 7 – Regression Coefficients of the polynomial surface of the stack power at 0.5 A/cm^2.

c_0	c_1	c_2	c_3
−2.79E+03	−1.10E+03	−9.03E+02	1.60E+03
c_4	c_5	c_6	c_7
7.45E+03	−2.76E+02	1.68E−01	1.28E+02
c_8	c_9	c_{10}	c_{11}
5.71E+03	−5.06E+03	−3.72E+03	2.54E+03
c_{12}	c_{13}	c_{14}	c_{15}
−1.44E+03	−3.11E+03	4.29E+03	2.48E−02
c_{16}	c_{17}	c_{18}	c_{19}
−2.02E+00	5.57E+03	−4.89E+02	2.29E+03
c_{20}	c_{21}	c_{22}	c_{23}
3.86E+03	−3.33E+03	−1.70E−01	4.11E+01
c_{24}	c_{25}	c_{26}	c_{27}
1.21E+04	−1.18E+04	1.39E+04	5.80E+03
c_{28}	c_{29}	c_{30}	c_{31}
1.50E−03	−7.63E+01	1.43E+04	−1.31E+04
c_{32}	c_{33}	c_{34}	c_{35}
−2.80E+04	7.61E+03	−2.23E−01	9.49E+01
c_{36}	c_{37}	c_{38}	c_{39}
8.12E+03	7.76E+03	6.11E−02	−1.26E+02
c_{40}	c_{41}	c_{42}	c_{43}
7.34E+03	1.05E+04	5.98E−04	−2.79E−01
c_{44}	c_{45}	c_{46}	c_{47}
2.39E−01	−2.06E−01	3.35E+01	−4.22E+01
c_{48}	c_{49}		
−1.74E+04	4.40E+02		

change in each point but the relative weight doesn't, so that the relative importance of each sensor is the same in every range of probability. For this reason, the sensitivity at a probability level of CDF = 0.5 are reported as representative for the sensitivities at each other probability level.

In Fig. 7 the sensitivities of the stack power to the input (and measurable) variables are shown at the current densities of 0.3, 0.5 and 0.7 [A/cm^2] respectively. It's important to underline that sensitivities are functions of the selected probability level, i.e. functions of a particular value of the CDF.

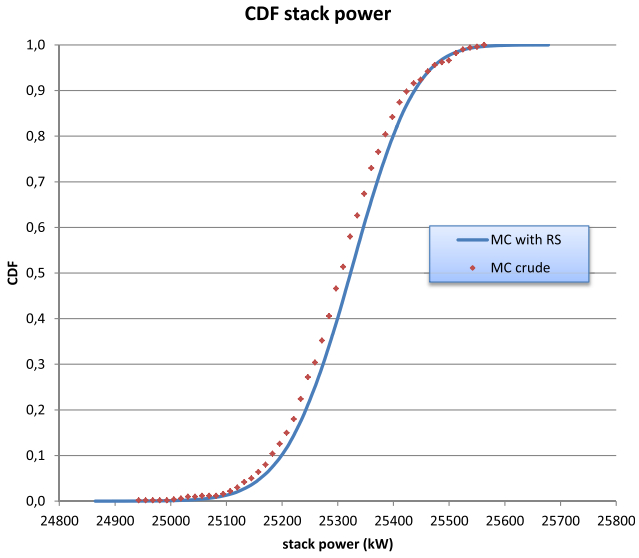

Fig. 6 – CDF of the stack power, in case of crude MC and MC with RS.

Exploring different probability levels is necessary in order to assess the real influence of a basic variable; for this reason in Fig. 7 each variable is characterized by three different values of sensitivities related to a low probability level (CFD = 0.001), an average probability level (CFD = 0.5) and a high probability level (CFD = 0.999).

For what concerns the effects on the stack power, at low current density (0.3 A/cm^2) the signal with the highest impact is the temperature of the anode inlet to the stack (T_{an_in}), while at high density current (0.7 A/cm^2) the most important signal is the temperature of the cathode inlet to the stack (T_{ca_in}). At mean current density (0.5 A/cm^2), it is possible to see that the values of sensitivity are almost equal. These signals (T_{an_in} and T_{ca_in}) deserve special attention since they corresponds to 80% of the total stack power sensitivity for low and high current density. A particular case is seen at low currents density and high probability, where the ambient temperature (t_{amb}) shows 50% of impact over the stack power (see Fig. 7). The sensitivities of the signals of the anode pressure, the anode mass flow, the cathode pressure, the cathode mass flow, the water cooling temperature, the water cooling pressure and the ambient temperature, reveal that the uncertainty in these quantities does not affect much the stack power.

The results demonstrate that accurate temperature sensors and sensor calibration are of significant importance for the control of the stack power. The selection of the correct sensor resolution for a fuel cell system application is a task to be cautiously carried out. The sensitivity analysis helps to determine the required characteristics (such as accuracy, redundancies or resolutions) of every sensor. Starting with a tolerated uncertainty, the sensor tolerances could be calculated.

Therefore the methodology and the results could provide a valuable tool for fuel cell control under uncertainty.

Conclusion

The introduction of new and innovative systems in aeronautics is a problematic issue because of the very strict safety requirements an aircraft system is subject to, even during experimental flight. Designers need to be able to predict failure scenarios to guarantee safety conditions, and to be able to extend the range of application of the innovative system.

In this paper, a possible application of reliability assessment for a hydrogen fuel cell aircraft, combining dynamic modeling and structural reliability techniques, has been presented. In particular the analysis is carried out for sensors failures, but the methods are widely applicable to other aspects of the reliability analysis. Sensors were chosen because they constitute the basis of the FC control system, which is extremely important for this innovative powertrain system.

The dynamic model developed by the authors proved to be accurate since it has been validated through several real flight tests of an FC powered two-seat ultra-light aircraft, in the framework of the EU funded ENFICA-FC Project.

The main outcomes are the following:

1. The use of the proposed uncertainty/sensitivity analysis to improve the failure analysis: the sensitivity analysis

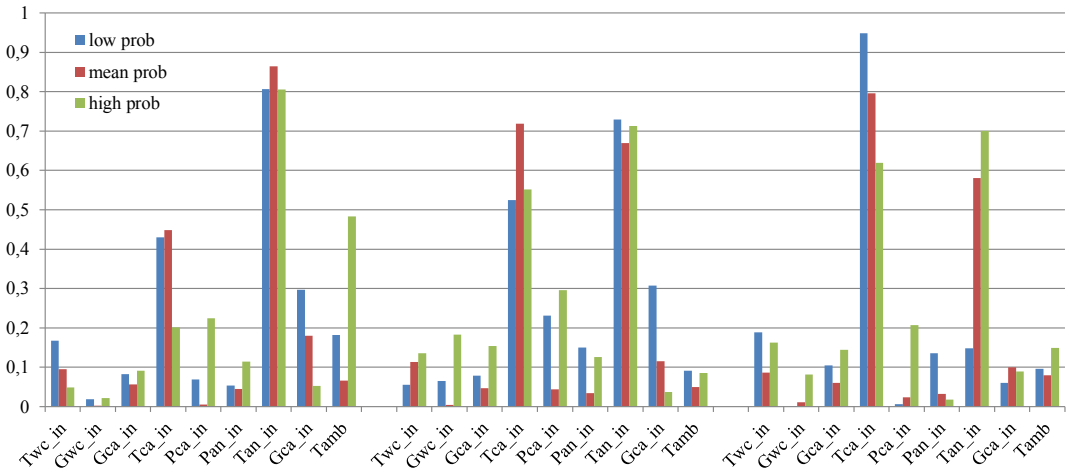

Fig. 7 – Sensitivity of the stack power towards the main control parameters @ 0.3, 0.5 & 0.7 A/cm^2.

provides useful information to engineers for developing a system, as well as appropriate sensor control characteristics;

2. The results demonstrate that accurate temperature sensors and sensor calibration are of unavoidable importance for the control of the stack temperature, over systems such as PEM fuel cells;
3. As an example in terms of power control of the system: the sensor signal with the highest impact on the stack power is the temperature of the cathode and anode inlet into the stack (T_{ca_in} & T_{an_in});
4. The time consuming simulations of the Monte Carlo method took around 420 min when only a single cycle of the 300 s for only one current density was run, while that RSM took a few seconds. Therefore, for model of complex systems, the most important advantage of RSM is the low computational effort it requires;
5. The presented method can easily integrate more complex model (i.e. simulations done with commercial finite element codes) of the elements of the power system; in this case the response surface generation is affected, but once generated the computational effort of the probabilistic analysis is totally unaffected.

Acknowledgments

The activity has been developed within the ENFICA-FC project. The Authors acknowledge the important contribution of European Commission by the funding programme ENFICA-FC, EC 6th FP – Contract No. AST5-CT-2006-030779.

REFERENCES

[1] Lapeña-Rey N, Mosquera J, Bataller E, Ortí F. First fuel-cell manned aircraft. J Aircr 2010;47(6).

[2] DLR. Fuel cells power first takeoff for DLR's antares aircraft. Fuel Cells Bull 2009;2009(9):3.

[3] Romeo G, Borello F, Correa G, Cestino E. ENFICA-FC: design of transport aircraft powered by fuel cell & flight test of zero emission 2-seater aircraft powered by fuel cells fueled by hydrogen. Int J Hydrogen Energy 2013;38(1):469–79.

[4] Yalcinoza T, Alama M. Improved dynamic performance of hybrid PEM fuel cells and ultracapacitors for portable application. Int J Hydrogen Energy 2008;33(7):1932–40.

[5] Rossi F, Nicolini A. Ethanol reforming for supplying molten carbonate fuel cells. Int J Low Carbon Tech 2013;8(2):140–5.

[6] Rossi F, Nicolini A. Experimental investigation on a novel electrolyte configuration for cylindrical molten carbonate fuel cells. J Fuel Cell Sci Tech 2011;8(5):1–9.

[7] Cleghorn SJC, Ren X, Springer TE, Wilson MS, Zawodzinski C, Zawodzinski TA, et al. PEM fuel cells for transportation and stationary power generation applications. Int J Hydrogen Energy 1997;22(12):1137–44.

[8] Barbir F, Fuchs M, Husar A, Neutzler J. Design and operational characteristics of automotive PEM fuel cell stacks. SAE 2000 World Congress. 2000.

[9] Zhang J, Wu J, Zhang H, Zhang J. PEM fuel cell testing and diagnosis. Amsterdam: Elsevier; 2013.

[10] Venkatasubramanian V, Rengaswamy R, Yin K, Kavuri S. A review of process fault detection and diagnosis: part I: quantitative model-based methods. Comput Chem Eng 2003;27(3):293–311.

[11] Gerbec M, Jovan V, Petrovcic J. Operational and safety analyses of a commercial PEMFC system. Int J Hydrogen Energy 2008;33:4147–60.

[12] Du Z, Jin X. Multiple faults diagnosis for sensors in air handling unit using fisher discriminant analysis. Energ Convers Manage 2008;49(12):3654–65.

[13] Åström K, Fontel E, Virtanen S. Reliability analysis and initial requirements for FC systems and stacks. J Power Sources 2007;171(1):46–54.

[14] Mawardi A, Pitchumani R. Effects of parameter uncertainty on the performance variability of proton exchange membrane (PEM) fuel cells. J Power Sources 2006;160(1):232–45.

[15] Placca L, Kouta R, Blachot J, Charon W. Effects of temperature uncertainty on the performance of a degrading PEM fuel cell model. J Power Sources 2009;194(1):313–27.

[16] Noorkami M, Robinson J, Meyer Q, Obeisun O, Fraga E, Reisch T, et al. Effect of temperature uncertainty on polymer electrolyte fuel cell performance. Int J Hydrogen Energy 2014;39(3):1439–48.
[17] Romeo G, Borello F, Correa G. Set-up and test flights of an all-electric 2-seater aeroplane powered by fuel cells. J Aircr 2011;49(8).
[18] Romeo G, Cestino E, Correa G, Borello F. A fuel cell based propulsion system for general aviation aircraft: the ENFICA-FC experience. SAE Int J Aerosp 2011;4(2):724–37.
[19] Correa G, Borello F, Santarelli M. Sensitivity analysis of temperature uncertainty in an aircraft PEM fuel cell. Int J Hydrogen Energy 2011;36(22):14745–58.
[20] Romeo G, Correa G, Borello F, Cestino E, Santarelli M. Air cooling of a 2-seater fuel cells powered aircraft: dynamic modelling and comparisons with experimental data. J Aerosp Eng 2012;25(3):356–68.
[21] Romeo G, Cestino E, Borello F, Correa G. Engineering method for air-cooling design of 2-seat propeller driven aircraft powered by fuel cells. J Aerosp Eng 2011;24:79–88.
[22] Romeo G, Cestino E, Pacino M, Borello F, Correa G. The design, manufacturing and testing of a propeller for a 2-seater aircraft powered by fuel cells, PART G. J Aerosp Eng 2012;226:804–16.
[23] Correa G, Santarelli M, Borello F, Cestino E, Romeo G. Flight test validation of the dynamic model of a fuel cell system for ultra-light aircraft. Proc Inst Mech Eng G J Aerosp Eng 2015;229(5):917–32.
[24] Adcock P, Kells A, Jackson C. PEM fuel cells for road vehicles. In: International Advanced Mobility Forum, EET-2008 European Ele-Drive Conference, Geneva; 2008.
[25] Hayter D. Fuel cell hybrid London taxi. In: Eleventh Grove Fuel Cell Symposium. London: Elsevier; 2009.
[26] Muller EA, Stefanopoulou AG. Analysis, modeling, and validation for the thermal dynamics of a polymer electrolyte membrane fuel cell system. J Fuel Cell Sci Tech 2006;3(2):99–110.
[27] Barendrecht E, Blomen MNMMJ. Electrochemistry of fuel cells. In: Fuel Cell Systems. New York: Plenum Press; 1993.
[28] Prentice G. Electrochemical engineering principles. Houston, USA: Prentice Hall International; 1991.
[29] Santarelli M, Torchio M, Cochis P. Parameters estimation of a PEM fuel cell polarization curve and analysis of their behavior with temperature. J Power Sources 2006;159:824–83.
[30] Zawodzinski T, Neeman M, Sillerud L, Gottesfeld S. Determination of water diffusion coefficients in perfluorosulfonate ionomeric membranes. J Phys Chem 1991;95:6040.
[31] Pukrushpan JT, Peng H, Stefanopoulou AG. Control-oriented modeling and analysis for automotive fuel cell systems. J Dyn Syst Meas Control Trans ASME 2004;126:14–25.
[32] Amphlett J, Baumert R, Mann R, Peppley B, Roberge P. Performance modeling of the Ballard Mark IV solid polymer electrolyte fuel cell, I. Mechanistic model development. J Electrochem Soc 1995;142(1):1–8.
[33] Bernardi D, Verbrugge M. Mathematical model of a gas diffusion electrode bonded to a polymer electrolyte. AIChE J 1991;37(8):1151–63.
[34] Amphlett J, Mann R, Peppley B, Thurgood C. Application of Butler–Volmer equations in the modelling of activation polarization for PEM fuel cells. J Power Sources October 2006;161(2):775–81.
[35] Springer T, Zawodzinski T, Gottesfeld S. Polymer electrolyte fuel cell model. J Electrochem Soc 1991;138:2334–41.
[36] Bernardi D, Dawn M. Water-balance calculations for solid-polymer-electrolyte fuel cells. J Electrochem Soc 1990;137:3344–50.
[37] Fuller T, Newman J. Experimental determination of the transport number of water in Nafion 117 membrane. J. Electrochem Soc 1992;139:1332–7.
[38] Wang Z, Wang C, Chen K. Two-phase flow and transport in the air cathode of proton exchange membrane fuel cells. J Power Sources 2001;94:40–50.
[39] Verbrugge M, Schneider E, Conell R, Hill R. The effect of temperature on the equilibrium and transport properties of saturated Poly(perfluorosulfonic acid) membranes. J Electrochem Soc 1992;139:3421.
[40] Frulla G, Borello F. In: Hayworth GI, editor. Structural reliability aspects for advanced composite material applications. Turin: Reliability Engineering Advances; 2009. p. 1–36.
[41] Iman RL, Davenport JM, Zeigler DK. Latin hypercube sampling (program user's guide). Technical Report SAND 79–1473. Albuquerque: Sandia National laboratories; 1980.
[42] Press W, Teukolsky S, Vetterling W, Flannery B. Numerical recipes in C: the art of scientific computing. 2nd ed. New York: Cambridge University Press; 1992.